# Distinctive associations between plasma p-tau181 levels and hippocampal subfield volume across the Alzheimer's disease continuum

Adea **Rich**,[1]* Hwamee **Oh**,[2,3]*

for the Alzheimer's Disease Neuroimaging Initiative[†]

[1]Brown University School of Public Health

[2]Departments of Psychiatry and Human Behavior and Cognitive and Psychological Sciences, Brown University

[3]Carney Institute for Brain Science, Brown University

*Corresponding authors:

Adea Rich, Department of Neurology, Columbia University Irving Medical Center, 710 W 168th St, New York, NY 10032, USA. E-mail: arr2251@cumc.columbia.edu or adea_rich@alumni.brown.edu

Hwamee Oh, Departments of Psychiatry and Human Behavior and Cognitive and Psychological Sciences, Brown University, 700 Butler Drive, Providence, RI 02906, USA. E-mail: hwamee_oh@brown.edu

**Abstract: Background:** Plasma p-tau181 is a promising diagnostic marker of Alzheimer's disease (AD) pathology, reflecting amyloid accumulation, tau deposition, and downstream neurodegeneration that leads to cognitive impairment. However, the specificity of plasma p-tau181 to AD-related tau pathology remains unclear. **Objective:** To assess whether plasma p-tau181 is differentially associated with volumetric changes in distinct hippocampal subfields and whether they mediate the relationship between plasma p-tau181 and cognition across the AD continuum. **Methods:** 213 participants with normal cognition (N=57), mild cognitive impairment (N=109), and AD (N=47) from the Alzheimer's Disease Neuroimaging Initiative (ADNI) were included for cross-sectional analyses of hippocampal subfield volume that was quantified using the Automatic Segmentation of Hippocampal Subfields (ASHS) software. A subset (n=89) was evaluated for one-year longitudinal changes in hippocampal subfield volume. **Results:** Higher plasma p-tau181 levels (pg/mL) were associated with decreased volumes in the CA1 and dentate gyrus, bilaterally, and right entorhinal cortex ($ps < 0.05$). Additionally, volumes of these subfields partially mediated the relationship between plasma p-tau181 and ADNI memory and executive function composite scores. Baseline plasma p-tau181, however, did not predict longitudinal atrophy of hippocampal subfields across diagnostic groups. **Conclusions:** Plasma p-tau181 is differentially associated with hippocampal subfields that are closely related to both age- and AD-related neurodegeneration. Elevated plasma p-tau181 levels may reflect tau accumulation, and volumetric changes in CA1 and DG may mediate the detrimental effect of tau pathology on cognition.

**Introduction**

Alzheimer's disease (AD)  is a neurodegenerative disorder pathologically characterized by the accumulation of extracellular amyloid-β (Aβ) plaques and intracellular neurofibrillary tangles (NFTs).[1] Recent advances in amyloid and tau positron emission tomography (PET), as well as Aβ42, phosphorylated-tau (p-tau), and total tau (t-tau) measured in cerebrospinal fluid (CSF),  have been shown to accurately detect these neuropathological features.[2–5] Structural magnetic resonance imaging (MRI) is also a widely validated biomarker for assessing atrophy in the medial temporal lobe, reflecting dendritic and neuronal damage associated with AD.[6–8] While PET and CSF markers of Aβ and tau have improved diagnostic accuracy for prodromal and dementia stages of AD, there remains a need for non-invasive, cost-effective, and accessible biomarkers that offer high sensitivity and specificity for both clinical and research settings.[9] Moreover, abnormal levels of Aβ and hyperphosphorylated tau (p-tau) pathologies begin to accumulate 15-20 years before symptom onset.[10,11] Considering the prolonged preclinical phase of AD, the availability of cost-effective and scalable biomarkers that can assist diagnosis and prognosis for such at-risk populations will be crucial for early diagnosis of the disease.[12]

Several blood-based plasma markers have been developed and assessed to validate their diagnostic and prognostic capabilities.[13–25] These markers include Aβ40, Aβ42, t-tau, different isoforms of p-tau, such as p-tau181, p-tau217, and p-tau231, and neurofilament light chain (NfL), which show a varying degree of diagnostic and prognostic capabilities along the AD continuum.[26–28] In particular, the plasma biomarkers p-tau181, p-tau217, and p-tau231 have emerged as promising indicators of Aβ and tau pathologies in AD.[29–31] Plasma levels of p-tau181, p-tau217, and p-tau231 have been shown to increase with cognitive decline, hippocampal atrophy, and the intensity of Aβ and tau pathologies.[32–36] Additionally, these biomarkers effectively distinguish between individuals with AD and healthy controls.[37] All three p-tau measures, however, correlate more strongly with amyloid PET than with tau PET, with p-tau217 demonstrating the strongest correlation, followed by p-tau231 and then p-tau181.[38]

Moreover, compared to p-tau181, plasma p-tau217 and p-tau231 show earlier and stronger associations with Aβ as well as tau pathologies, becoming abnormal in Aβ-positive, and tau-negative (preclinical AD) individuals.[21,33,34,39,40] Plasma p-tau217 is particularly accurate in diagnosing AD dementia and can distinguish AD from primary age-related tauopathy (PART) and mixed AD pathologies, outperforming plasma p-tau181.[41] While plasma p-tau231 and p-tau217 show earlier changes in preclinical AD, plasma p-tau181 remains frequently used in clinical trials and is strongly correlated with both amyloid pathology and cognitive decline.[34,42–44] Although soluble p-tau plasma measures are considered as a promising AD biomarker and are interpreted as reflecting tau pathology, concentrations of p-tau have shown stronger associations with Aβ deposition than tau pathology, especially in cognitively unimpaired individuals.[38,45] Therefore, it remains unclear to what extent plasma p-tau measures reflect tau neurofibrillary tangles in the brain, especially in the early stage of AD pathologies.

Increased plasma p-tau181 has been linked to hippocampal atrophy,[46–48] while hippocampal (HC) subfields has been implicated for differential susceptibility to AD.[49–51] The HC formation includes the entorhinal cortex (ERC), subiculum (SUB), cornu ammonis regions (CA1-3), and dentate gyrus (DG), each structurally diverse with distinct functions and varying disease susceptibility.[52–55] In AD, atrophy predominantly affects the ERC, CA1, and SUB, while the DG and CA3 are often spared.[50,56,57] In healthy aging, atrophy typically occurs in DG and CA3.[58] Examining HC subfield integrity in association with plasma p-tau181 may improve the detection of subtle AD-related structural changes and their cognitive implications,[59,60] while clarifying how plasma p-tau181 specifically relates to tau pathology that could exert its downstream effects, such as hippocampal atrophy and cognitive decline.[61,62] Examining the specific relationship between plasma p-tau181 and hippocampal subfield integrity, thus, will help to gain a more comprehensive understanding of the diagnostic and prognostic capabilities of plasma p-tau181.

In this study, we examined how plasma p-tau181 was associated with HC subfield volume across diagnostic groups (cognitively normal, mild cognitive impairment, and AD) and

assessed whether baseline plasma p-tau181 could predict HC volumetric changes between baseline and a one-year follow-up. Additionally, we examined whether HC subfield volume mediated the associations between plasma p-tau181 and cognition. We hypothesized that elevated plasma p-tau181 levels would be associated with greater atrophy in CA1, ERC, and SUB across the AD continuum—subfields particularly vulnerable in AD compared to normal aging—and that these subfields would mediate the relationship between plasma p-tau181 and both memory and executive function.

**Methods**

*Study participants*

Participants were selected from the Alzheimer's Disease Neuroimaging Initiative (ADNI) database (https://adni.loni.usc.edu/). ADNI, initiated in 2003, is a longitudinal multicenter study collecting clinical, imaging, genetic, and biochemical biomarker data to aid in the understanding of AD.[63] The project obtained approval from the institutional review boards of all collaborating institutions, and written informed consent was obtained from all participants.

In this study, participants who were classified as cognitively normal (CN) or cognitively impaired, including those with mild cognitive impairment (MCI), and AD dementia, were included. A total of 213 participants with plasma p-tau181 measurements and high-resolution T2-weighted MRI scans available at baseline were selected from the ADNI database. Subsequent HC subfield volume collected around 1 year later was measured for 89 participants. A detailed description of the sample selection can be found in Figure 1. Additional information regarding eligible participants can be found at https://adni.loni.usc.edu/data-samples/adni-data/.
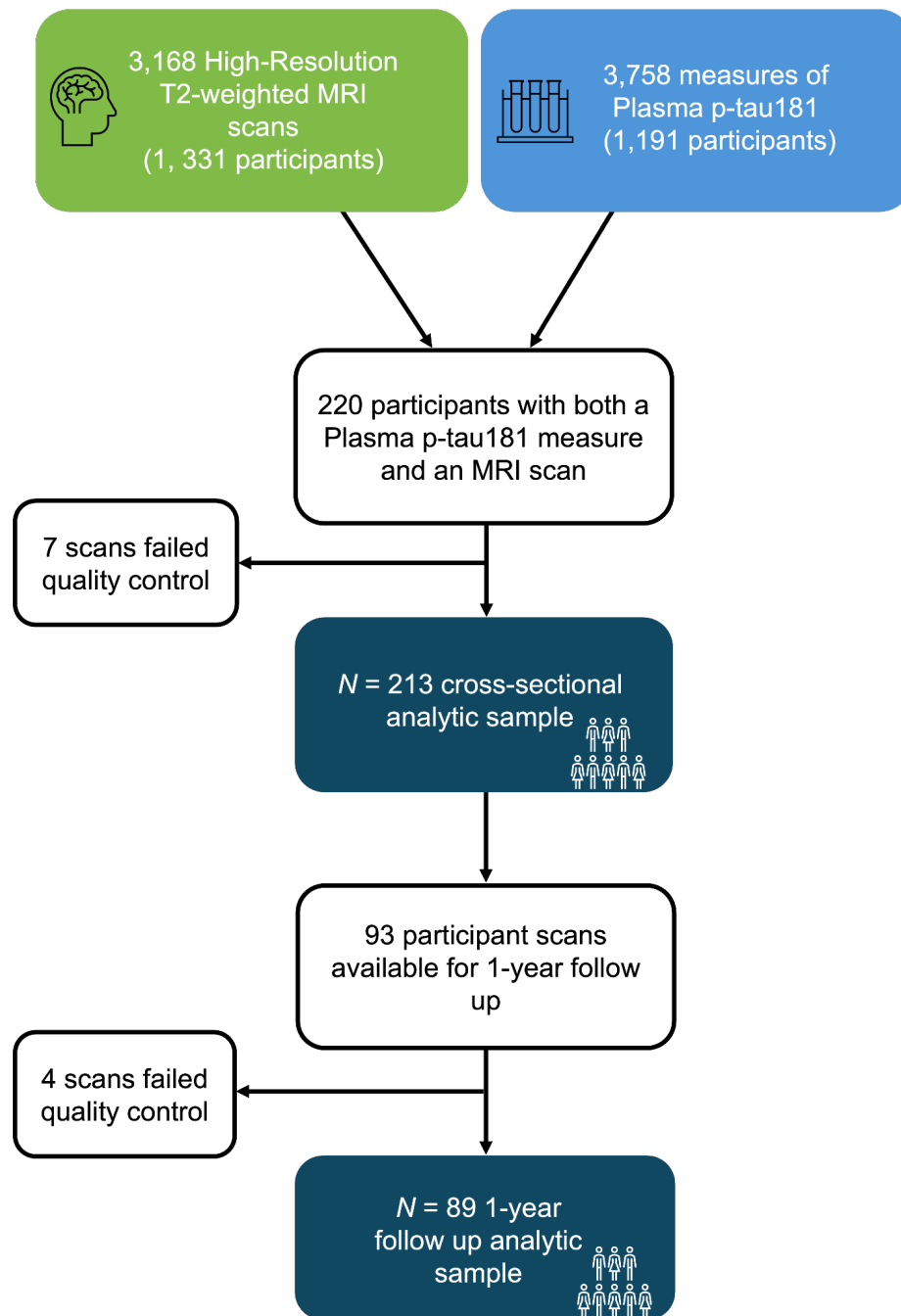
Figure 1. Sample selection from the Alzheimer's Disease Neuroimaging Initiative (ADNI). 213 participants were selected based on availability of p-tau measures and qualified MRI data cross-sectionally and for the 1-year follow-up.

*Image acquisition*

T1-weighted high-resolution MRI scans and T2-weighted hippocampal subfield scans were obtained from various scanners at multiple ADNI sites. Up-to-date information on MRI imaging protocols can be accessed at https://adni.loni.usc.edu/data-samples/adni-data/neuroimaging/mri/.

*Automatic Segmentation of Hippocampal Subfields*

We measured HC subfield volumes using the Automatic Segmentation of Hippocampal Subfields (ASHS) software.[64] The ASHS segments the HC subfields based on a multi-atlas segmentation approach with joint label fusion and bias correction using advanced machine-learning techniques. ASHS is a fully automated framework that includes MRI pre-processing, image segmentation, bias correction, and refinement. It utilizes both high-resolution T1-weighted and T2-weighted images to achieve optimal segmentation and divides the medial temporal lobe into the following subfields: cornu ammonia 1 (CA1), cornu ammonis 2 (CA2), cornu ammonis 3 (CA3), dentate gyrus (DG), subiculum (SUB), entorhinal cortex (ERC), perirhinal cortex of Brodmann area 35 and Brodmann area 36, collateral sulcus, and a miscellaneous part (cysts and cerebrospinal fluid). More information on ASHS and a comparison with the manual approach and FreeSurfer version 6.0 can be found elsewhere.[64]

The volumes of HC subfields used in this analysis (CA1-CA3, DG, ERC, and SUB) were normalized by dividing the raw volumes by the number of slices in which the regions of interest (ROI) appear.[64] The rate of change for HC subfield volume was calculated by subtracting the adjusted volume at baseline from the adjusted volume at year one and dividing by the time in years between these two measurements. Larger negative values indicate greater atrophy over the (approximately one year) time between data collection.

*Plasma p-tau181*

Plasma p-tau181 data were obtained from the ADNI database. Plasma p-tau181 was processed using the clinically validated Single Molecule array (Simoa) HD-X (Quanterix) technique developed at the Clinical Neurochemistry Laboratory, University of Gothenburg, Sweden, as previously described.[48] This assay utilizes the AT270 monoclonal antibody specific to the threonine-181 phosphorylation site, along with the detection anti-tau mouse monoclonal antibody Tau12, to measure N-terminal to mid-domain forms of p-tau181. The quantification range for this assay, after dilution correction, is between 1.0 and 128.0 pg/mL.

*Cognitive testing*

We analyzed ADNI-MEM, a composite memory score based on the Rey Auditory Verbal Learning Task (AVLT), ADAS-COG-13, Mini-Mental State Examination (MMSE), and Logical Memory tasks, as well as ADNI-EF, a composite executive functioning score based on the WAIS-R Digit Symbol Substitution, Digit Span Backwards, Trails A and B, Category Fluency, and Clock Drawing.[65,66] Higher scores indicate better cognitive performance for both ADNI-MEM and EF.

*Statistical analyses*

Statistical analyses were carried out in R version 4.2.2.[67] Differences among diagnostic groups (CN, MCI, AD) in demographic and clinical characteristics were evaluated using analysis of variance (ANOVA) for numeric variables, the chi-squared test for categorical variables in the cross-sectional sample, and Fisher's exact test for categorical variables in the 1-year follow-up sample. Differences in HC subfield volumes among diagnostic groups were assessed using analysis of covariance (ANCOVA) and Tukey's HSD, controlling for age and sex. A linear regression model evaluated the baseline association between plasma p-tau181 concentration

and diagnostic groups, adjusting for age and sex. Marginal means were obtained, and Tukey's HSD assessed pairwise differences, controlling for family-wise error. Another linear regression model examined the association between plasma p-tau181 concentration and HC subfield volume across diagnostic groups, adjusted for age and sex, with adjusted p-values calculated using the Benjamini-Hochberg method to control the false discovery rate (FDR) and account for multiple comparisons. Additionally, a linear regression model assessed baseline plasma p-tau181 concentration and the rate of change in HC subfield volume, adjusted for time (in years), age, and sex. Finally, a mediation analysis determined whether the association between baseline plasma p-tau181 concentration and composite scores for memory and executive function are mediated by HC subfield volume, adjusting for age, sex, and years of education, with bootstrapped 95% confidence intervals. Missing data comprised < 5% for all variables and was handled using complete case analysis.[68] Statistical significance was defined as $p < 0.05$.

**Results**

*Demographic and clinical characteristics*

The demographic and clinical characteristics of the participants are summarized in Table 1. Demographic characteristics, including age, education, and sex, did not significantly differ between diagnostic groups in the cross-sectional and 1-year follow-up samples. However, significant differences in clinical characteristics were observed for plasma p-tau181, MMSE, APOE4-carrier status, memory composite score, and executive function composite score among the CN, MCI, and AD groups in both samples ($p < 0.05$). The AD group consisted of more APOE4 carriers and higher plasma p-tau181 levels, and showed lower MMSE, memory composite, and executive function composite scores.

HC subfield volume for CA1, DG, ERC, and SUB significantly differed among the CN, MCI, and AD groups in both the cross-sectional and 1-year follow-up samples ($p < 0.001$), with the AD group showing lower volumes. Right CA2 also significantly differed among groups in

both samples ($p < 0.01$), while left CA2 volume did not show significant differences. Likewise,

left CA3 volume did not significantly differ among groups. Right CA3 volume significantly

differed among groups in the cross-sectional sample ($p < 0.05$) but did not in the 1-year follow-

up sample.

Table 1. Demographic and clinical characteristics of subjects

| | Cross-sectional sample | | | | | 1-year follow-up sample | | | | |
|---|---|---|---|---|---|---|---|---|---|---|
| | Total (N=213) | CN (N=57) | MCI (N=109) | AD (N=47) | p-value | Total (N=89) | CN (N=26) | MCI (N=54) | AD (N=9) | p-value |
| Sex | | | | | 0.32 | | | | | 0.35 |
| Female | 98 (46%) | 26 (46%) | 46 (42%) | 26 (55%) | | 38 (43%) | 8 (31%) | 26 (48%) | 4 (44%) | |
| Male | 115 (54%) | 31 (54%) | 63 (58%) | 21 (45%) | | 51 (57%) | 18 (69%) | 28 (52%) | 5 (56%) | |
| Age | 73.84 (7.82) | 74.32 (7.43) | 73.44 (7.78) | 74.17 (8.45) | 0.75 | 73.90 (7.95) | 74.50 (8.02) | 74.22 (7.99) | 70.22 (7.38) | 0.34 |
| Education | 16.45 (2.60) | 16.53 (2.56) | 16.56 (2.71) | 16.09 (2.40) | 0.56 | 16.57 (2.71) | 16.38 (2.77) | 16.70 (2.70) | 16.33 (2.83) | 0.85 |
| APOE4 | | | | | <0.001 | | | | | <0.05 |
| Non-carriers | 121 (57%) | 43 (75%) | 65 (60%) | 13 (28%) | | 48 (54%) | 18 (69%) | 28 (52%) | 2 (22%) | |
| Carriers | 92 (43%) | 14 (25%) | 44 (40%) | 34 (72%) | | 41 (46%) | 8 (31%) | 26 (48%) | 7 (78%) | |
| MMSE | 26.68 (4.01) | 29.00 (1.27) | 27.83 (2.23) | 21.26 (4.50) | <0.001 | 27.40 (3.23) | 29.08 (0.93) | 27.74 (1.82) | 20.56 (5.22) | <0.001 |
| ADNI-MEM | 0.36 (1.14) | 1.24 (0.69) | 0.53 (0.84) | -1.10 (0.70) | <0.001 | 0.51 (1.03) | 1.12 (0.71) | 0.50 (0.87) | -1.23 (0.66) | <0.001 |
| ADNI-EF | 0.29 (1.19) | 0.98 (0.85) | 0.48 (0.95) | -0.99 (1.10) | <0.001 | 0.50 (1.11) | 1.00 (0.80) | 0.50 (1.01) | -0.98 (1.16) | <0.001 |
| P-tau 181 (pg/mL) | 18.99 (12.99) | 14.58 (8.81) | 17.25 (10.58) | 28.36 (17.29) | <0.001 | 17.60 (11.30) | 12.48 (8.66) | 18.36 (11.39) | 27.85 (10.10) | <0.01 |
| Right CA1 (mm³) | 56.40 (11.03) | 62.57 (7.78) | 57.38 (10.18) | 46.64 (9.83) | <0.001 | 56.04 (11.09) | 63.12 (7.95) | 54.99 (10.06) | 41.90 (9.54) | <0.001 |
| Right CA2 (mm³) | 1.91 (0.63) | 2.23 (0.44) | 1.85 (0.65) | 1.66 (0.65) | <0.001 | 1.92 (0.63) | 2.17 (0.67) | 1.87 (0.57) | 1.39 (0.58) | <0.01 |
| Right CA3 (mm³) | 8.78 (4.01) | 8.31 (2.47) | 9.47 (4.57) | 7.75 (3.90) | <0.05 | 8.72 (4.49) | 9.09 (4.95) | 8.54 (4.01) | 8.73 (5.75) | 0.88 |
| Right DG (mm³) | 42.56 (10.32) | 48.18 (8.49) | 43.15 (9.55) | 34.38 (8.97) | <0.001 | 42.37 (11.44) | 47.40 (8.40) | 41.91 (11.31) | 30.59 (11.48) | <0.001 |
| Right ERC (mm³) | 35.56 (8.87) | 40.05 (7.56) | 35.64 (8.56) | 29.92 (7.98) | <0.001 | 35.73 (8.57) | 40.52 (6.13) | 35.20 (8.17) | 25.06 (6.57) | <0.001 |
| Right SUB (mm³) | 21.37 (4.19) | 23.30 (2.99) | 22.02 (3.73) | 17.52 (4.01) | <0.001 | 21.15 (3.93) | 23.19 (3.30) | 20.94 (3.66) | 16.57 (3.12) | <0.001 |
| Left CA1 (mm³) | 54.16 (10.21) | 59.97 (6.98) | 55.05 (9.30) | 45.08 (9.49) | <0.001 | 54.76 (10.52) | 61.57 (6.42) | 53.83 (9.90) | 40.64 (7.53) | <0.001 |
| Left CA2 (mm³) | 2.59 (0.56) | 2.70 (0.40) | 2.55 (0.60) | 2.54 (0.63) | 0.23 | 2.54 (0.51) | 2.68 (0.44) | 2.54 (0.55) | 2.23 (0.32) | 0.08 |
| Left CA3 (mm³) | 8.40 (3.55) | 8.31 (3.38) | 8.11 (3.31) | 9.21 (4.19) | 0.20 | 7.64 (3.22) | 7.59 (2.22) | 7.65 (3.46) | 7.71 (4.35) | 0.10 |
| Left DG (mm³) | 40.41 (9.93) | 45.33 (7.96) | 40.97 (9.83) | 33.16 (8.12) | <0.001 | 40.86 (10.72) | 45.90 (8.59) | 40.03 (10.97) | 31.26 (6.82) | <0.001 |
| Left ERC (mm³) | 36.69 (8.25) | 40.02 (6.69) | 37.66 (8.28) | 30.40 (6.43) | <0.001 | 36.84 (8.11) | 41.16 (5.65) | 36.14 (8.20) | 28.55 (6.00) | <0.001 |
| Left SUB (mm³) | 21.32 (4.12) | 23.09 (3.40) | 21.80 (3.93) | 18.06 (3.54) | <0.001 | 21.65 (4.33) | 24.32 (3.73) | 21.08 (4.02) | 17.40 (3.23) | <0.001 |

Mean (SD) for continuous variables; n (%) for categorical variables. Abbreviations: CN, Cognitively Normal; MCI, Mild Cognitive Impairment; APOE4, *apolipoprotein E4*; MMSE, Mini-Mental State Examination; ADNI-MEM, Memory composite score; ADNI-EF, Executive Functioning composite score. CA1, Cornu ammonis 1; CA2, Cornu ammonis 2; CA3, Cornu ammonis 3; DG, Dentate gyrus; SUB, Subiculum; ERC, Entorhinal cortex

*Hippocampal subfield volume differences among diagnostic groups*

Group differences in HC subfield volume among diagnostic groups are presented in Figure 2. Significant differences were observed in CA1, DG, and right ERC subfields among all diagnostic groups ($p < 0.01$), with the MCI and AD groups exhibiting smaller volumes than the CN group. The AD group further demonstrated even smaller volumes than the MCI group. The left ERC and SUB displayed differences between the MCI and AD groups, and between the CN and AD groups ($p < 0.01$), with the AD group showing smaller volumes than the MCI and CN groups. The right CA2 demonstrated significant differences between the CN and MCI groups, and between the CN and AD groups ($p < 0.01$), with the AD group exhibiting smaller volumes than the CN group, and the MCI group exhibiting smaller volumes than the CN group. The right CA3 volume significantly differed between the MCI and AD groups ($p < 0.05$), with the AD group exhibiting lower volumes than the MCI group. The left CA2 and CA3 did not show significant differences among any diagnostic groups.
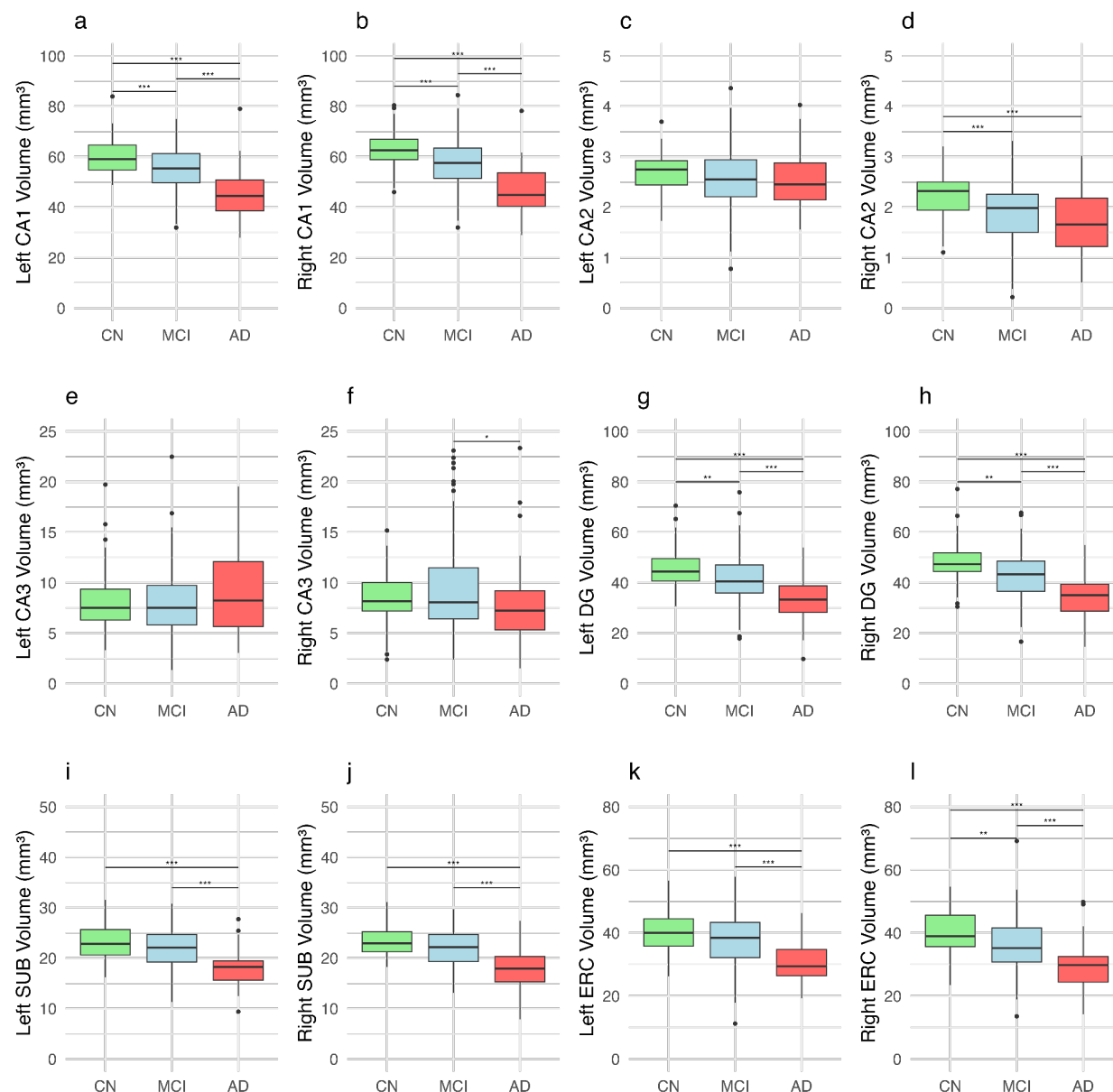
Figure 2. Hippocampal subfield volume differences among diagnostic groups. Panels a-l show the distribution of hippocampal subfield volumes across diagnostic groups. Each box represents the interquartile range (IQR) of the data, with the horizontal line inside the box representing the median. The 'whiskers' extend to 1.5 times the IQR above and below the upper and lower quartiles. Abbreviations: CN, Cognitively normal; MCI, Mild cognitive impairment; AD, Alzheimer's disease; CA1, Cornu ammonis 1; CA2, Cornu ammonis 2; CA3, Cornu ammonis 3; DG, Dentate gyrus; SUB, Subiculum; ERC, Entorhinal cortex. *($p < 0.05$), **($p < 0.01$), ***($p < 0.001$).

*Plasma p-tau181 level differences among diagnostic groups*

The estimated marginal means of plasma p-tau181 levels vary among diagnostic groups. Plasma p-tau181 levels are 14.3 pg/mL (95% CI: 11.3 - 17.4) for CN individuals, 17.1 pg/mL (95% CI: 14.8 - 19.3) for individuals with MCI, and 28.5 pg/mL (95% CI: 25.1 - 31.9) for individuals with AD. Pairwise comparisons revealed significant differences between CN and AD ($p < 0.001$) and between MCI and AD ($p < 0.001$), with the AD group having higher plasma p-tau181 concentrations. No significant difference was found between CN and MCI ($p = 0.34$).

*Baseline association between plasma p-tau181 and hippocampal subfield volume across diagnostic groups*

Associations between baseline plasma p-tau181 levels and HC subfield volume across diagnostic groups are illustrated in Figure 3. Our findings indicate that higher levels of plasma p-tau181 (pg/mL) are associated with smaller volumes in the left CA1 ($\beta = -0.119$, $p = 0.019$, Fig. 2a), right CA1 ($\beta = -0.154$, $p = 0.005$, Fig. 2b), left DG ($\beta = -0.120$, $p = 0.016$, Fig. 2g), right DG ($\beta = -0.146$, $p = 0.005$, Fig. 2h), and right ERC ($\beta = -0.091$, $p = 0.048$, Fig. 2i). In contrast, left CA2 ($\beta = 0.002$, $p = 0.491$, Fig. 2c), right CA2 ($\beta = -0.002$, $p = 0.494$, Fig. 2d), left CA3 ($\beta = 0.011$, $p = 0.559$, Fig. 2e), and right CA3 ($\beta = -0.007$, $p = 0.730$, Fig. 2f) do not show significant relationships with plasma p-tau181 across diagnostic groups. Similarly, the left SUB ($\beta = -0.012$, $p = 0.558$, Fig. 2i), right SUB ($\beta = -0.032$, $p = 0.144$, Fig. 2j), and left ERC ($\beta = -0.056$, $p = 0.188$, Fig. 2k) do not demonstrate significant relationships with plasma p-tau181 across diagnostic groups. After adjusting for multiple testing, the right CA1 and right DG ($p < 0.05$) remained statistically significant.
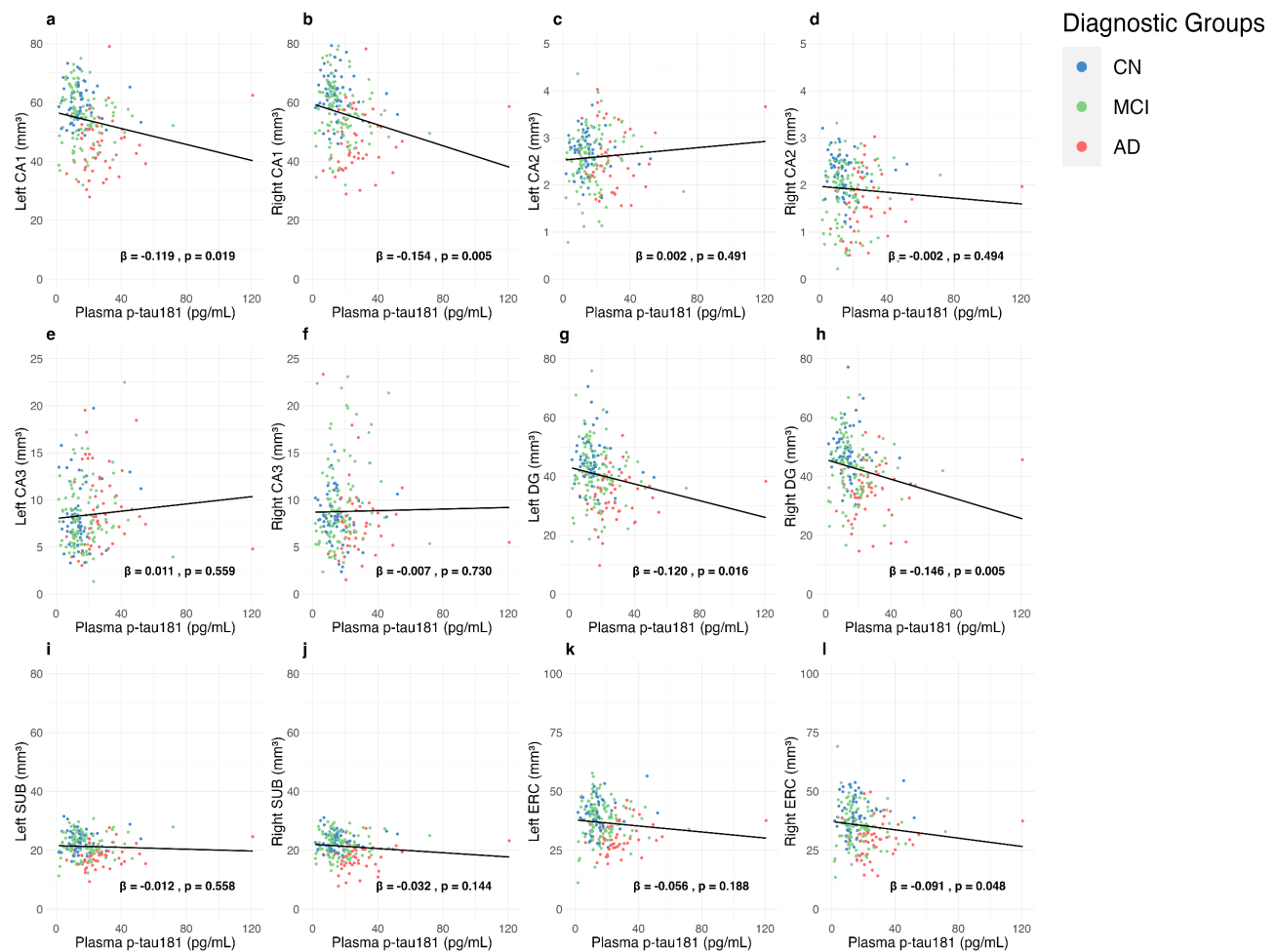
14

Figure 3. Baseline association between plasma p-tau181 and hippocampal subfield volume across diagnostic groups. *β* coefficients and *p*-values represent the regression model adjusted for age and sex. The scatter plot illustrates the relationship between plasma p-tau181 levels and hippocampal subfield volumes across diagnostic groups without covariates, with each point representing observed data and the line indicating the fitted multiple linear regression model. Abbreviations: CN, cognitively normal; MCI, mild cognitive impairment; AD, Alzheimer's disease; CA1, Cornu ammonis 1; CA2, Cornu ammonis 2; CA3, Cornu ammonis 3; DG, dentate gyrus; SUB, subiculum; ERC, entorhinal cortex.
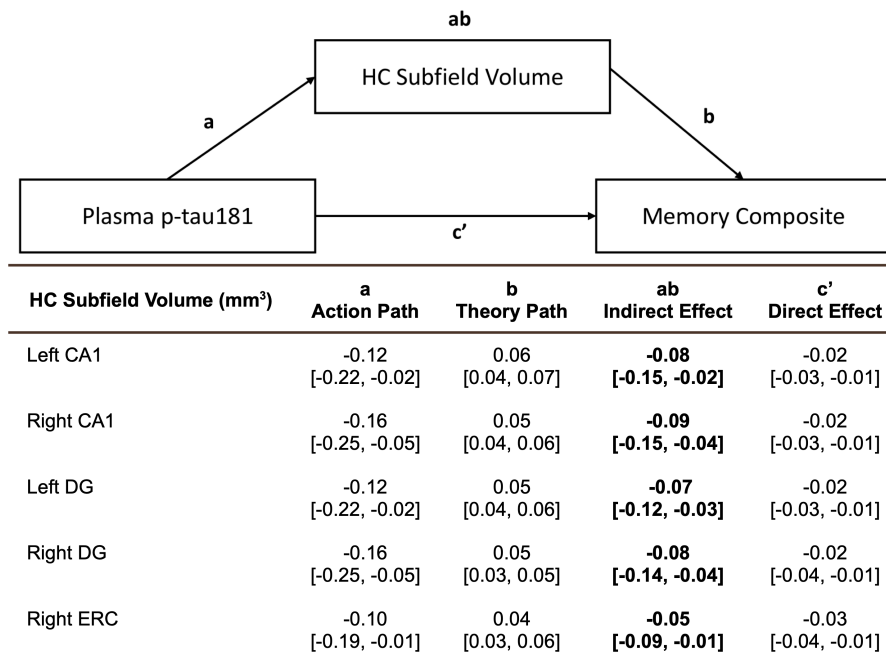
15

*Baseline plasma p-tau181 and hippocampal subfield volume rate of change*

There was no association between baseline plasma p-tau181 levels and the rate of change in HC subfield volume from baseline to the 1-year follow-up. Although no subfields demonstrated statistically significant results, several subfields exhibited negative beta values, potentially indicating atrophy over the year: left CA1 ($\beta$ = -0.020, $p$ = 0.561), left DG ($\beta$ = -0.100, $p$ = 0.109), right DG ($\beta$ = -0.083, $p$ = 0.191), left SUB ($\beta$ = -0.066, $p$ = 0.128), right SUB ($\beta$ = -0.061, $p$ = 0.170), left CA2 ($\beta$ = -0.002, $p$ = 0.726), and right CA2 ($\beta$ = -0.002, $p$ = 0.725, Fig. 2d), while other subfields did not exhibit negative beta values: right CA1 ($\beta$ = 0.019, $p$ = 0.657), left ERC ($\beta$ = 0.002, $p$ = 0.978), right ERC ($\beta$ = 0.036, $p$ = 0.462), and right CA3 ($\beta$ = 0.004, $p$ = 0.922).

*Mediation analysis*

Increased plasma p-tau181 concentration was significantly associated with both lower memory and executive function composite scores ($p$ < 0.001). Consequently, a mediation analysis was conducted to assess whether the relationship between plasma p-tau181 and composite scores in memory and executive function is mediated by HC subfield volume. The analysis revealed that CA1, DG, and right ERC volume partially mediate the association between plasma p-tau181 concentrations and both memory and executive function composite scores (Figure 4).

(a) Memory Composite



| HC Subfield Volume (mm³) | a Action Path | b Theory Path | ab Indirect Effect | c' Direct Effect |
|---|---|---|---|---|
| Left CA1 | -0.12 [-0.22, -0.02] | 0.06 [0.04, 0.07] | **-0.08 [-0.15, -0.02]** | -0.02 [-0.03, -0.01] |
| Right CA1 | -0.16 [-0.25, -0.05] | 0.05 [0.04, 0.06] | **-0.09 [-0.15, -0.04]** | -0.02 [-0.03, -0.01] |
| Left DG | -0.12 [-0.22, -0.02] | 0.05 [0.04, 0.06] | **-0.07 [-0.12, -0.03]** | -0.02 [-0.03, -0.01] |
| Right DG | -0.16 [-0.25, -0.05] | 0.05 [0.03, 0.05] | **-0.08 [-0.14, -0.04]** | -0.02 [-0.04, -0.01] |
| Right ERC | -0.10 [-0.19, -0.01] | 0.04 [0.03, 0.06] | **-0.05 [-0.09, -0.01]** | -0.03 [-0.04, -0.01] |

(b) Executive Functioning Composite



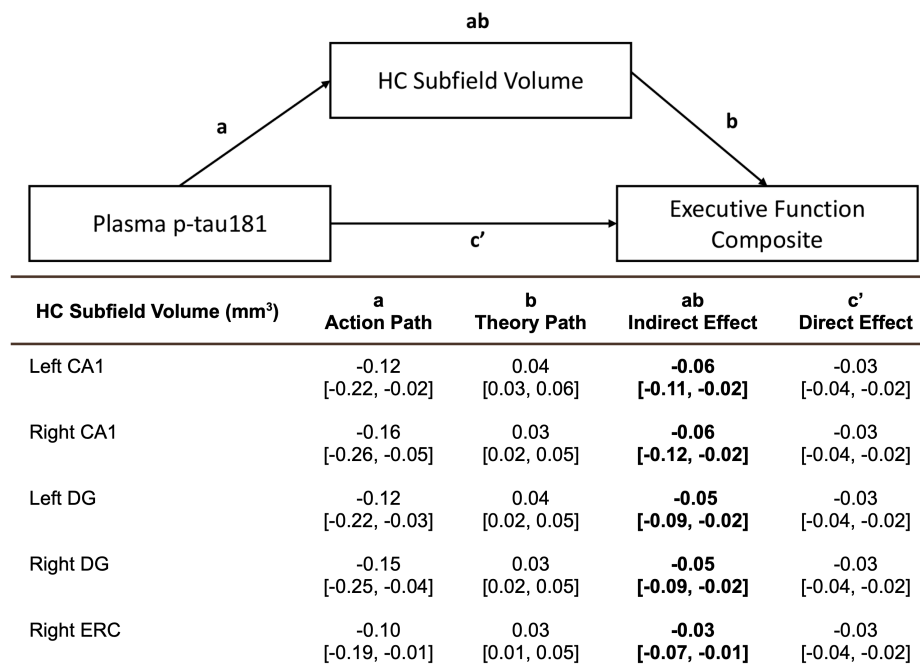| HC Subfield Volume (mm³) | a Action Path | b Theory Path | ab Indirect Effect | c' Direct Effect |
|---|---|---|---|---|
| Left CA1 | -0.12 [-0.22, -0.02] | 0.04 [0.03, 0.06] | **-0.06 [-0.11, -0.02]** | -0.03 [-0.04, -0.02] |
| Right CA1 | -0.16 [-0.26, -0.05] | 0.03 [0.02, 0.05] | **-0.06 [-0.12, -0.02]** | -0.03 [-0.04, -0.02] |
| Left DG | -0.12 [-0.22, -0.03] | 0.04 [0.02, 0.05] | **-0.05 [-0.09, -0.02]** | -0.03 [-0.04, -0.02] |
| Right DG | -0.15 [-0.25, -0.04] | 0.03 [0.02, 0.05] | **-0.05 [-0.09, -0.02]** | -0.03 [-0.04, -0.02] |
| Right ERC | -0.10 [-0.19, -0.01] | 0.03 [0.01, 0.05] | **-0.03 [-0.07, -0.01]** | -0.03 [-0.04, -0.02] |

Figure 4. Mediation Analysis. Completely standardized coefficient estimates are presented with bootstrapped 95% confidence intervals in brackets. Mediation analyses revealed a significant indirect effect of hippocampal subfield volume on the relationship between plasma p-tau181 and memory (a), as well as executive functioning (b). While the direct effects of plasma p-tau181 and composite scores were significant, our mediation model demonstrated that elevated plasma p-tau181 concentration was associated with lower hippocampal subfield volumes in CA1, DG, and right ERC, which were linked to lower memory and executive functioning composite scores. Abbreviations: CA1, Cornu ammonis 1; DG, Dentate gyrus; ERC, Entorhinal cortex.

17

**Discussion**

Accumulating evidence indicates that blood-based biomarkers can differentiate diagnostic status across the AD continuum, and they show a high correlation with the severity of AD neuropathologies such as brain Aβ deposition.[69,70] Among blood-based biomarkers, plasma p-tau181 has been associated with the disease severity of AD with high accuracy, indicating its potential role as a diagnostic biomarker of AD.[71] Despite its potential utility as a diagnostic biomarker of AD, its relationship with brain tau pathology and a neural mechanism underlying the linkage between plasma p-tau181 and cognitive impairment remain elusive. Based on the previous findings of specific relationships between HC subfields and AD,[52] we examined how plasma p-tau181 selectively relates to HC subfield volumes at baseline as well as atrophy over one year among older adults across different diagnostic groups (CN, MCI, and AD).

Major findings of the present study include: (1) higher plasma levels of p-tau181 were specifically associated with smaller volume of the CA1, DG, and right ERC cortex cross-sectionally; (2) the volume of these HC subfield regions partially mediated the relationship between plasma p-tau181 and cognitive performance in both memory and executive function; (3) baseline plasma p-tau181 did not predict longitudinal atrophy of the HC subfields. We further replicated that levels of plasma p-tau181 were higher with AD patients compared to CN subjects and that HC subfield volumes known to have differential vulnerabilities to AD pathology, such as the SUB, CA1, and ERC, showed lower volumes in AD groups compared to CN subjects.[71,72]

Our findings of a significant association between higher plasma p-tau181 levels and smaller volumes in CA1, DG, and right ERC subfields are in part consistent with previous research linking AD to volumetric loss in CA1 and ERC.[72,73] Based on prior evidence suggesting that DG is relatively resistant to AD pathology, we hypothesized that plasma p-tau181 would be associated with reduced CA1 volume, but not DG. In contrast to our prediction, our results did not reveal differential associations between plasma p-tau181 and DG or CA1 volumes across

18

the AD continuum. Interestingly, reductions in both CA1 and DG volumes have been linked to age-related memory decline in older adults, where CA1 integrity has been associated with lower cognitive function scores, and DG with difficulties in pattern separation.[50,57,74,75] These findings suggest that elevated plasma p-tau181 levels in association with the HC subfields may be more reflective of age-related neurodegenerative processes rather than AD-related tau pathology.

The significant relationship between plasma p-tau181 and DG volume may also point to a potential link with primary age-related tauopathy (PART), which typically involves tau deposition in the DG and CA4 subregions.[76,77] Conversely, NFTs in DG and CA4 are characteristic of advanced AD, and our findings may indicate neurodegeneration driven by tau pathology in ERC, which disrupts perforant pathway inputs to DG.[78] Interestingly, while the right ERC demonstrated a significant association with plasma p-tau181, the left ERC did not, and the overall significance observed in ERC was less pronounced compared to DG. Despite plasma p-tau181 being associated with widespread amyloidosis, our results indicate that the relationship between plasma p-tau181 and HC atrophy may closely reflect tau tangles rather than amyloid accumulation. While some studies found a significant association between plasma p-tau levels and temporal meta ROI tau PET levels, these studies included not only nondemented but also demented patients,[38] potentially indicating that the plasma p-tau levels might have reflected whole-cortex tau tangles in addition to the temporal lobe tau accumulation. Collectively, our results may indicate the link between plasma p-tau181 level and temporal lobe tau accumulation.

Contrary to our hypothesis, we did not observe an association between plasma p-tau181 levels and SUB volume. This finding contradicts existing research that suggests AD pathology and AD blood biomarkers typically correlate with decreased volume in the SUB.[79] It is plausible a biomarker more specific to AD pathology, such as p-tau217, may be better suited to detect AD-related structural changes. Overall, our findings of the differential association of plasma p-tau181 with HC subfield volume indicate that plasma p-tau181 may be

19

linked to neurodegeneration in both aging and AD, potentially reflecting tau accumulation in HC subfields.[80,81]

Additionally, we found that reduced volumes in CA1, DG, and right ERC partially mediate the relationship between plasma p-tau181 levels and cognitive performance in episodic memory and executive function. Higher plasma p-tau181 levels were associated with lower scores in both cognitive domains, with volumetric decline in these subfields contributing to this association. This is consistent with previous research showing that CA1 and DG mediate the relationship between AD pathology and memory recall and reconsolidation.[51] Another study found that larger CA1 and CA4-DG volumes predicted better executive function.[82] In our sample, reduced volumes in CA1 and DG more strongly mediated memory performance than executive function, while both domains were affected. Collectively, our results further support the conclusion that plasma p-tau181 may be associated with broader cognitive impairments,[42] including both memory performance, such as pattern separation linked to DG atrophy, and executive function.[53,83] It is important to note that tauopathy in the absence of Aβ pathology, as indicated by increased plasma p-tau181 levels without Aβ, was shown to predict neither cognitive decline nor hippocampal atrophy.[84] This suggests that Aβ pathology may be a necessary, although not sufficient, component in AD pathophysiology. Despite the absence of Aβ pathology, plasma p-tau181 significantly improved discrimination between Braak I–II and Braak 0 stages among both cognitively unimpaired and impaired individuals, as well as across all older adults combined.[85] Our findings extend the existing literature by identifying a role of hippocampal subfield volume in the relationship between plasma p-tau181 levels and cognitive impairment and may enhance our understanding of the cognitive difficulties associated with elevated plasma p-tau181 levels.

Baseline plasma p-tau181 levels did not predict longitudinal atrophy in the HC subfields over one year. Previous literature has shown an association between plasma p-tau181 and annual changes in overall HC volume.[32] However, plasma p-tau181 may not be sensitive

20

enough to detect subtle subfield-specific changes within shorter follow-up periods. In contrast, other AD biomarkers, such as p-tau217 and p-tau231, which exhibit more pronounced increases along the AD continuum, may be better suited for identifying these structural changes. A longer follow-up may be necessary to fully capture the predictive value of plasma p-tau181.

The current study has some limitations. The small sample size may have limited statistical power to detect subfield-specific associations in some HC subfields and restricted our ability to conduct separate analyses within diagnostic groups. Future research utilizing larger and more demographically representative samples could reveal additional relationships between pathology, brain volume, cognitive performance, and plasma biomarkers, particularly with minimal loss to follow-up and sufficient access to track longitudinal changes. Second, although we found a robust relationship between p-tau181 and the HC subfield volumes using the well-validated segmentation tool of the HC subfields, other promising p-tau variants, such as p-tau217 and p-tau231, should also be investigated, which may offer stronger clinical utility due to their ability to detect earlier changes in AD. However, these variants are not currently available in the ADNI dataset, so they could not be assessed as part of this study. Finally, incorporating neuropsychological assessments tailored to the cognitive tasks associated with each HC subfield could further elucidate the cognitive implications of plasma biomarkers.

Our study demonstrates that higher plasma p-tau181 levels are associated with lower volumes in CA1, DG, and right ERC subfields, with these volumes partially mediating the relationship between plasma p-tau181 and cognition. This suggests that plasma p-tau181 levels may indicate tau accumulation, with changes in CA1 and DG mediating the effect of tau pathology on cognition. Identifying which subfields correlate with plasma biomarkers could enhance our understanding of how blood-based plasma biomarkers reflect brain AD pathology and support their diagnostic capabilities. While further research is warranted to clarify these associations, our findings contribute to the growing body of literature examining the relationships between biomarkers, brain structure, and cognitive impairment.

**Author Contributions**

**Acknowledgments**

**Funding**

This study was supported by National Institute on Aging grant (R01-AG068990) to

H.O.

**Declaration of conflicting interest**

The authors declared no potential conflicts of interest with respect to the research,

authorship, and/or publication of this article

**Consent to participate**

This study was done using publicly obtainable secondary data. Informed consent was

obtained through the Alzheimer's Disease Neuroimaging Initiative.

**Data Availability**

The data supporting the findings of this study are openly available in [Ptau181_HC] at

[https://github.com/adearich/Ptau181_HC]. These data were derived from the following

resources available in the public domain: [https://adni.loni.usc.edu/].

References

1. DeTure MA, Dickson DW. The neuropathological diagnosis of Alzheimer's disease. *Mol Neurodegener* 2019; 14: 32.

2. Mankhong S, Kim S, Lee S, et al. Development of Alzheimer's Disease Biomarkers: From CSF- to Blood-Based Biomarkers. *Biomedicines* 2022; 10: 850.

3. Jack CR, Barrio JR, Kepe V. Cerebral amyloid PET imaging in Alzheimer's disease. *Acta Neuropathol (Berl)* 2013; 126: 643–657.

4. Keshavan A, Wellington H, Chen Z, et al. Concordance of CSF measures of Alzheimer's pathology with amyloid PET status in a preclinical cohort: A comparison of Lumipulse and established immunoassays. *Alzheimers Dement Diagn Assess Dis Monit* 2021; 13: e12131.

5. Marquié M, Normandin MD, Vanderburg CR, et al. Validating novel tau positron emission tomography tracer [F-18]-AV-1451 (T807) on postmortem brain tissue. *Ann Neurol* 2015; 78: 787–800.

6. Vemuri P, Jack CR. Role of structural MRI in Alzheimer's disease. *Alzheimers Res Ther* 2010; 2: 23.

7. Johnson KA, Fox NC, Sperling RA, et al. Brain Imaging in Alzheimer Disease. *Cold Spring Harb Perspect Med* 2012; 2: a006213–a006213.

8. Frisoni GB, Fox NC, Jack CR, et al. The clinical use of structural MRI in Alzheimer disease. *Nat Rev Neurol* 2010; 6: 67–77.

9. Blennow K, Galasko D, Perneczky R, et al. The potential clinical value of plasma biomarkers in Alzheimer's disease. *Alzheimers Dement* 2023; 19: 5805–5816.

10. Vermunt L, Sikkes SAM, Van Den Hout A, et al. Duration of preclinical, prodromal, and dementia stages of Alzheimer's disease in relation to age, sex, and *APOE* genotype. *Alzheimers Dement* 2019; 15: 888–898.

11. Jack CR, Knopman DS, Jagust WJ, et al. Tracking pathophysiological processes in Alzheimer's disease: an updated hypothetical model of dynamic biomarkers. *Lancet Neurol* 2013; 12: 207–216.

12. Rafii MS, Aisen PS. Detection and treatment of Alzheimer's disease in its preclinical stage. *Nat Aging* 2023; 3: 520–531.

13. Simrén J, Leuzy A, Karikari TK, et al. The diagnostic and prognostic capabilities of plasma biomarkers in Alzheimer's disease. *Alzheimers Dement J Alzheimers Assoc* 2021; 17: 1145–1156.

14. Mendes AJ, Ribaldi F, Lathuiliere A, et al. Head-to-head study of diagnostic accuracy of plasma and cerebrospinal fluid p-tau217 versus p-tau181 and p-tau231 in a memory clinic cohort. *J Neurol* 2024; 271: 2053–2066.

15. Sanchez E, Wilkinson T, Coughlan GT, et al. Association of plasma biomarkers with

cognitive domains across three neurodegenerative diseases and cerebrovascular disease. *Alzheimers Dement* 2023; 19: e079139.

16. Kwon HS, Lee E, Kim H, et al. Predicting amyloid PET positivity using plasma p-tau181 and other blood-based biomarkers. *Alzheimers Dement Diagn Assess Dis Monit* 2023; 15: e12502.

17. Mielke MM, Frank RD, Dage JL, et al. Comparison of Plasma Phosphorylated Tau Species With Amyloid and Tau Positron Emission Tomography, Neurodegeneration, Vascular Pathology, and Cognitive Outcomes. *JAMA Neurol* 2021; 78: 1108.

18. Therriault J, Benedet AL, González Escalante A, et al. Plasma biomarkers as stand-alone tests in the diagnosis of Alzheimer's disease. *Alzheimers Dement* 2023; 19: e080181.

19. Baiardi S, Quadalti C, Mammana A, et al. Diagnostic value of plasma p-tau181, NfL, and GFAP in a clinical setting cohort of prevalent neurodegenerative dementias. *Alzheimers Res Ther* 2022; 14: 153.

20. Janelidze S, Mattsson N, Palmqvist S, et al. Plasma P-tau181 in Alzheimer's disease: relationship to other biomarkers, differential diagnosis, neuropathology and longitudinal progression to Alzheimer's dementia. *Nat Med* 2020; 26: 379–386.

21. Palmqvist S, Janelidze S, Quiroz YT, et al. Discriminative Accuracy of Plasma Phospho-tau217 for Alzheimer Disease vs Other Neurodegenerative Disorders. *JAMA* 2020; 324: 772.

22. Barthélemy NR, Horie K, Sato C, et al. Blood plasma phosphorylated-tau isoforms track CNS change in Alzheimer's disease. *J Exp Med* 2020; 217: e20200861.

23. Ashton NJ, Puig-Pijoan A, Milà-Alomà M, et al. Plasma and CSF biomarkers in a memory clinic: Head-to-head comparison of phosphorylated tau immunoassays. *Alzheimers Dement* 2023; 19: 1913–1924.

24. Coomans EM, Verberk IMW, Ossenkoppele R, et al. A Head-to-Head Comparison Between Plasma pTau181 and Tau PET Along the Alzheimer's Disease Continuum. *J Nucl Med* 2023; 64: 437–443.

25. Yakoub Y, Ashton NJ, Strikwerda-Brown C, et al. Longitudinal blood biomarker trajectories in preclinical Alzheimer's disease. *Alzheimers Dement* 2023; 19: 5620–5631.

26. Janelidze S, Bali D, Ashton NJ, et al. Head-to-head comparison of 10 plasma phospho-tau assays in prodromal Alzheimer's disease. *Brain* 2023; 146: 1592–1601.

27. Janelidze S, Teunissen CE, Zetterberg H, et al. Head-to-Head Comparison of 8 Plasma Amyloid-β 42/40 Assays in Alzheimer Disease. *JAMA Neurol* 2021; 78: 1375.

28. Dong Y, Hou T, Li Y, et al. Plasma Amyloid-β, Total Tau, and Neurofilament Light Chain Across the Alzheimer's Disease Clinical Spectrum: A Population-Based Study. *J Alzheimers Dis* 2023; 96: 845–858.

29. Smirnov DS, Ashton NJ, Blennow K, et al. Plasma biomarkers for Alzheimer's Disease in

relation to neuropathology and cognitive change. *Acta Neuropathol (Berl)* 2022; 143: 487–503.

30. Mattsson-Carlgren N, Janelidze S, Palmqvist S, et al. Longitudinal plasma p-tau217 is increased in early stages of Alzheimer's disease. *Brain* 2020; 143: 3234–3241.

31. Mielke MM, Dage JL, Frank RD, et al. Performance of plasma phosphorylated tau 181 and 217 in the community. *Nat Med* 2022; 28: 1398–1405.

32. Wang Y-L, Chen J, Du Z-L, et al. Plasma p-tau181 Level Predicts Neurodegeneration and Progression to Alzheimer's Dementia: A Longitudinal Study. *Front Neurol* 2021; 12: 695696.

33. Ashton NJ, Pascoal TA, Karikari TK, et al. Plasma p-tau231: a new biomarker for incipient Alzheimer's disease pathology. *Acta Neuropathol (Berl)* 2021; 141: 709–724.

34. Milà-Alomà M, Ashton NJ, Shekari M, et al. Plasma p-tau231 and p-tau217 as state markers of amyloid-β pathology in preclinical Alzheimer's disease. *Nat Med*. Epub ahead of print 11 August 2022. DOI: 10.1038/s41591-022-01925-w.

35. Bucci M, Bluma M, Savitcheva I, et al. Profiling of plasma biomarkers in the context of memory assessment in a tertiary memory clinic. *Transl Psychiatry* 2023; 13: 268.

36. Chatterjee P, Pedrini S, Ashton NJ, et al. Diagnostic and prognostic plasma biomarkers for preclinical Alzheimer's disease. *Alzheimers Dement* 2022; 18: 1141–1154.

37. Bayoumy S, Verberk IMW, Den Dulk B, et al. Clinical and analytical comparison of six Simoa assays for plasma P-tau isoforms P-tau181, P-tau217, and P-tau231. *Alzheimers Res Ther* 2021; 13: 198.

38. Therriault J, Vermeiren M, Servaes S, et al. Association of Phosphorylated Tau Biomarkers With Amyloid Positron Emission Tomography vs Tau Positron Emission Tomography. *JAMA Neurol* 2023; 80: 188.

39. Brickman AM, Manly JJ, Honig LS, et al. Plasma p-tau181, p-tau217, and other blood-based Alzheimer's disease biomarkers in a multi-ethnic, community study. *Alzheimers Dement* 2021; 17: 1353–1364.

40. Suárez-Calvet M, Karikari TK, Ashton NJ, et al. Novel tau biomarkers phosphorylated at T181, T217 or T231 rise in the initial stages of the preclinical Alzheimer's *continuum* when only subtle changes in Aβ pathology are detected. *EMBO Mol Med* 2020; 12: e12921.

41. Yu L, Boyle PA, Janelidze S, et al. Plasma p-tau181 and p-tau217 in discriminating PART, AD and other key neuropathologies in older adults. *Acta Neuropathol (Berl)* 2023; 146: 1–11.

42. Xiao Z, Wu X, Wu W, et al. Plasma biomarker profiles and the correlation with cognitive function across the clinical spectrum of Alzheimer's disease. *Alzheimers Res Ther* 2021; 13: 123.

43. Mammel A, Kumar P, Fortna R, et al. pTau181 plasma biomarker performance as an inclusion criterion for Alzheimer's Disease clinical trials. *Alzheimers Dement* 2023; 19:

e077053.

44. Tropea TF, Waligorska T, Xie SX, et al. Plasma phosphorylated tau181 predicts cognitive and functional decline. *Ann Clin Transl Neurol* 2023; 10: 18–31.

45. Mattsson-Carlgren N, Janelidze S, Bateman RJ, et al. Soluble P-tau217 reflects amyloid and tau pathology and mediates the association of amyloid with tau. *EMBO Mol Med* 2021; 13: e14022.

46. Pereira JB, Janelidze S, Stomrud E, et al. Plasma markers predict changes in amyloid, tau, atrophy and cognition in non-demented subjects. *Brain* 2021; 144: 2826–2836.

47. Chong JR, Ashton NJ, Karikari TK, et al. Plasma P-tau181 to Aβ42 ratio is associated with brain amyloid burden and hippocampal atrophy in an Asian cohort of Alzheimer's disease patients with concomitant cerebrovascular disease. *Alzheimers Dement* 2021; 17: 1649–1662.

48. Karikari TK, Pascoal TA, Ashton NJ, et al. Blood phosphorylated tau 181 as a biomarker for Alzheimer's disease: a diagnostic performance and prediction modelling study using data from four prospective cohorts. *Lancet Neurol* 2020; 19: 422–433.

49. La Joie R, Perrotin A, De La Sayette V, et al. Hippocampal subfield volumetry in mild cognitive impairment, Alzheimer's disease and semantic dementia. *NeuroImage Clin* 2013; 3: 155–162.

50. Mueller SG, Schuff N, Yaffe K, et al. Hippocampal atrophy patterns in mild cognitive impairment and Alzheimer's disease. *Hum Brain Mapp* 2010; 31: 1339–1347.

51. Adams JN, Márquez F, Larson MS, et al. Differential involvement of hippocampal subfields in the relationship between Alzheimer's pathology and memory interference in older adults. *Alzheimers Dement Diagn Assess Dis Monit* 2023; 15: e12419.

52. Small SA, Schobel SA, Buxton RB, et al. A pathophysiological framework of hippocampal dysfunction in ageing and disease. *Nat Rev Neurosci* 2011; 12: 585–601.

53. Mueller SG, Chao LL, Berman B, et al. Evidence for functional specialization of hippocampal subfields detected by MR subfield volumetry on high resolution images at 4 T. *NeuroImage* 2011; 56: 851–857.

54. Tamnes CK, Walhovd KB, Engvig A, et al. Regional Hippocampal Volumes and Development Predict Learning and Memory. *Dev Neurosci* 2014; 36: 161–174.

55. Maruszak A, Thuret S. Why looking at the whole hippocampus is not enough-a critical role for anteroposterior axis, subfield and activation analyses to enhance predictive value of hippocampal changes for Alzheimer's disease diagnosis. *Front Cell Neurosci*; 8. Epub ahead of print 31 March 2014. DOI: 10.3389/fncel.2014.00095.

56. West MJ, Coleman PD, Flood DG, et al. Differences in the pattern of hippocampal neuronal loss in normal ageing and Alzheimer's disease. *The Lancet* 1994; 344: 769–772.

57. Mueller SG, Weiner MW. Selective effect of age, Apo e4, and Alzheimer's disease on

hippocampal subfields. *Hippocampus* 2009; 19: 558–564.

58. Pereira JB, Valls-Pedret C, Ros E, et al. Regional vulnerability of hippocampal subfields to aging measured by structural and diffusion MRI. *Hippocampus* 2014; 24: 403–414.

59. Carlesimo GA, Piras F, Orfei MD, et al. Atrophy of presubiculum and subiculum is the earliest hippocampal anatomical marker of Alzheimer's disease. *Alzheimers Dement Diagn Assess Dis Monit* 2015; 1: 24–32.

60. De Flores R, La Joie R, Chételat G. Structural imaging of hippocampal subfields in healthy aging and Alzheimer's disease. *Neuroscience* 2015; 309: 29–50.

61. La Joie R, Visani AV, Baker SL, et al. Prospective longitudinal atrophy in Alzheimer's disease correlates with the intensity and topography of baseline tau-PET. *Sci Transl Med* 2020; 12: eaau5732.

62. Biel D, Brendel M, Rubinski A, et al. Tau-PET and in vivo Braak-staging as prognostic markers of future cognitive decline in cognitively normal to demented individuals. *Alzheimers Res Ther* 2021; 13: 137.

63. Mueller SG, Weiner MW, Thal LJ, et al. The Alzheimer's Disease Neuroimaging Initiative. *Neuroimaging Clin N Am* 2005; 15: 869–877.

64. Yushkevich PA, Pluta JB, Wang H, et al. Automated volumetry and regional thickness analysis of hippocampal subfields and medial temporal cortical structures in mild cognitive impairment: Automatic Morphometry of MTL Subfields in MCI. *Hum Brain Mapp* 2015; 36: 258–287.

65. Crane PK, Carle A, Gibbons LE, et al. Development and assessment of a composite score for memory in the Alzheimer's Disease Neuroimaging Initiative (ADNI). *Brain Imaging Behav* 2012; 6: 502–516.

66. Gibbons LE, Carle AC, Mackin RS, et al. A composite score for executive functioning, validated in Alzheimer's Disease Neuroimaging Initiative (ADNI) participants with baseline mild cognitive impairment. *Brain Imaging Behav* 2012; 6: 517–527.

67. R Core Team. R: A language and environment for statistical computing. Vienna, Austria: R Foundation for Statistical Computing; 2021. Available from: https://www.R-project.org/.

68. Graham JW. Missing Data Analysis: Making It Work in the Real World. *Annu Rev Psychol* 2009; 60: 549–576.

69. Guo Y, Shen X-N, Wang H-F, et al. The dynamics of plasma biomarkers across the Alzheimer's continuum. *Alzheimers Res Ther* 2023; 15: 31.

70. Rudolph MD, Sutphen CL, Register TC, et al. Associations among plasma, MRI, and amyloid PET biomarkers of Alzheimer's disease and related dementias and the impact of health-related comorbidities in a community-dwelling cohort. *Alzheimers Dement* 2024; 20: 4159–4173.

71. Mielke MM, Hagen CE, Xu J, et al. Plasma phospho-tau181 increases with Alzheimer's

disease clinical severity and is associated with tau-PET and amyloid-PET. *Alzheimers Dement J Alzheimers Assoc* 2018; 14: 989–997.

72. Bobinski M, De Leon MJ, Tarnawski M, et al. Neuronal and volume loss in CA1 of the hippocampal formation uniquely predicts duration and severity of Alzheimer disease. *Brain Res* 1998; 805: 267–269.

73. Price JL, Ko AI, Wade MJ, et al. Neuron Number in the Entorhinal Cortex and CA1 in Preclinical Alzheimer Disease. *Arch Neurol* 2001; 58: 1395.

74. Yassa MA, Lacy JW, Stark SM, et al. Pattern separation deficits associated with increased hippocampal CA3 and dentate gyrus activity in nondemented older adults. *Hippocampus* 2011; 21: 968–979.

75. Shing YL, Rodrigue KM, Kennedy KM, et al. Hippocampal Subfield Volumes: Age, Vascular Risk, and Correlation with Associative Memory. *Front Aging Neurosci*; 3. Epub ahead of print 2011. DOI: 10.3389/fnagi.2011.00002.

76. Crary JF, Trojanowski JQ, Schneider JA, et al. Primary age-related tauopathy (PART): a common pathology associated with human aging. *Acta Neuropathol (Berl)* 2014; 128: 755–766.

77. Kim D, Kim H-S, Choi S-M, et al. Primary Age-Related Tauopathy: An Elderly Brain Pathology Frequently Encountered during Autopsy. *J Pathol Transl Med* 2019; 53: 159–163.

78. Witter MP. The perforant path: projections from the entorhinal cortex to the dentate gyrus. In: *Progress in Brain Research*. Elsevier, pp. 43–61.

79. Cao J, Tang Y, Chen S, et al. The Hippocampal Subfield Volume Reduction and Plasma Biomarker Changes in Mild Cognitive Impairment and Alzheimer's Disease. *J Alzheimers Dis* 2024; 98: 907–923.

80. Saunders TS, Pozzolo FE, Heslegrave A, et al. Predictive blood biomarkers and brain changes associated with age-related cognitive decline. *Brain Commun* 2023; 5: fcad113.

81. for the Alzheimer's Disease Neuroimaging Initiative, Tissot C, L. Benedet A, et al. Plasma pTau181 predicts cortical brain atrophy in aging and Alzheimer's disease. *Alzheimers Res Ther* 2021; 13: 69.

82. Salling ZN, Szymkowicz SM, Dotson VM. 58 Hippocampal Subregions Predict Executive Function Across the Adult Lifespan. *J Int Neuropsychol Soc* 2023; 29: 466–467.

83. Bakker A, Kirwan CB, Miller M, et al. Pattern Separation in the Human Hippocampal CA3 and Dentate Gyrus. *Science* 2008; 319: 1640–1642.

84. Oberstein TJ, Schmidt MA, Florvaag A, et al. Amyloid-β levels and cognitive trajectories in non-demented pTau181-positive subjects without amyloidopathy. *Brain* 2022; 145: 4032–4041.

85. Jack CR, Wiste HJ, Algeciras-Schimnich A, et al. Predicting amyloid PET and tau PET stages with plasma biomarkers. *Brain* 2023; 146: 2029–2044.